The interaction of entropy fluctuations with turbine blade rows; a mechanism of turbojet engine noise

By N. A. Cumpsty† and F. E. Marble‡

† *Whittle Laboratory, University Engineering Department, Madingley Road, Cambridge CB3 0EL, UK.*

‡ *Division of Engineering and Applied Science, California Institute of Technology, California, U.S.A.*

The theory relating to the interaction of entropy fluctuations ('hot spots'), as well as vorticity and pressure, with blade rows is described. A basic feature of the model is that the blade rows have blades of sufficiently short chord that this is negligible in comparison with the wavelength of the disturbances. For the interaction of entropy with a blade row to be important, it is essential that the steady pressure change across the blade row should be large, although all unsteady perturbations are assumed small.

A number of idealized examples have been calculated, beginning with isolated blade rows, progressing to single and then to several turbine stages. Finally, the model has been used to predict the low-frequency rearward-radiated acoustic power from a commercial turbojet engine. Following several assumptions, together with considerable empirical data, the correct trend and level are predicted, suggesting the mechanism to be important at low jet velocities.

1. Introduction

It is now generally accepted that jet propulsion engines produce more noise from their exhaust than can be accounted for by jet noise alone. The situation can be schematically illustrated by figure 1. As the jet velocity is reduced, the jet noise drops rapidly (being approximately proportional to V_{j}^8) whereas the engine noise source drops very much more slowly. In fact the level of the pure jet noise actually varies in a somewhat more complicated fashion than shown, because of variations in temperature, but the indicated trends remain correct. The extra noise is known variously as excess, tailpipe or core noise and becomes important only at low jet velocities; the effect of forward aircraft speed reduces the jet noise and therefore increases the relative importance of other sources.

Over the last few years evidence has begun to indicate that much of the extra noise coming from the exhaust of the engine is associated with the combuster. In particular, Hoch & Hawkins (1973) reported a significant change in noise when the combuster design on the same engine was changed from cannular

(separate chambers discharging into an annulus before entering the turbine) to an annular design (no separate chambers). The high-frequency noise associated with turbine tones at blade-passing frequency was increased, but the low-frequency noise was reduced. It is this low-frequency noise that is the subject of the present paper. More recently, Mathews & Peracchio (1974) measured pressure fluctuations in one of the eight combustion chambers of an engine and obtained a significant cross-correlation between this and the noise in the far field of the engine. The peak of the cross-correlation occurred at about 400 Hz, which in the present context is low frequency.
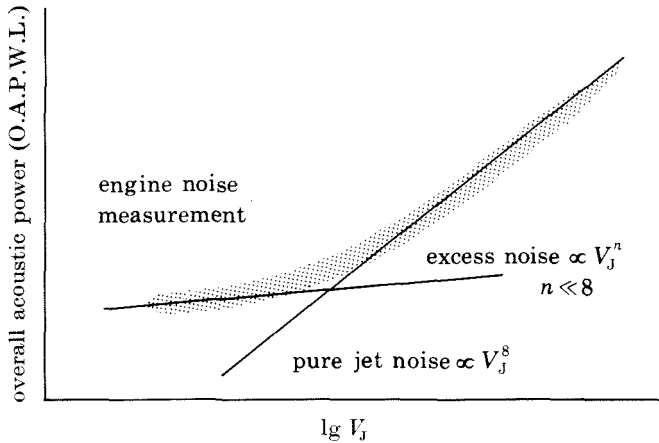

FIGURE 1. Schematic representation of variation of rear arc noise from a jet engine with jet velocity.

The existence of a significant cross-correlation, however, does not show more than the contribution of the combustion system to the core noise, and there are currently two different views as to the basic mechanism by which this involvement occurs. The conceptually simpler view is that the fluctuating heat release produces fluctuations in pressure which propagate through the turbine and are radiated to the far field. In contrast, the model assumed in the present paper is that the fluctuating heat release produces a variation in entropy, and that pressure fluctuations are produced as this inhomogeneity is convected through the turbine.

The problem of resolving whether the main source is direct combustion noise or the indirect noise due to entropy interacting with the turbine is a difficult one. A simple one-dimensional analysis for the effect of a fluctuating heat release shows that the production of entropy and pressure fluctuations are inextricably connected. Furthermore, the entropy fluctuations interact with the turbine nozzles so that pressure waves are propagated back into the combustor. The nozzles into the turbine are choked, or nearly choked, and a one-dimensional analysis of the interaction of entropy fluctuations with a choked nozzle indicates that the upstream pressure fluctuation has essentially the same amplitude and functional

dependence on combustion region Mach number as the pressure fluctuation produced directly by fluctuating heat release. Pressure measurements in the combuster do not therefore offer any direct check on the applicability of either model. The present work concentrates on the indirect mechanism, and endeavours to establish the validity of the model by predicting the level and spectrum of the excess engine noise.

The present model uses the concept of the compact nozzle, introduced by Marble (1973), Marble & Candel (1977), where the interaction of entropy and pressure waves with choked and unchoked nozzles is developed. It is important to draw the distinction between entropy and temperature fluctuations because the perturbation in temperature, T', is made up ot two parts, the entropy perturbation, s', and the isentropic temperature change consequent upon the pressure perturbation, p'. The full perturbation in temperature can be written in non-dimensional form as

$$T'/T = s'/c_p + (\gamma - 1)\,(p'/\gamma p).$$

The salient new features of the present model for considering series of turbine blade rows, together with some of their ramifications, are as follows:

(*a*) The blade passages are assumed sufficiently short compared with the wavelength that there is no phase difference between the flow quantities on the upstream and downstream sides of the blade row. The flow inside the blade row may therefore be treated as steady, and solutions upstream and downstream may be obtained by matching mass flow, total pressure and entropy across the row. For frequencies below about 1 kHz (at which the acoustic wavelength at turbine inlet is about $\frac{3}{4}$ m) this assumption is likely to be very good even for large engines, except for Mach numbers in the passages very close to one.

(*b*) The blade pitch–chord ratio is assumed to be low, which is equivalent to assuming that the blades are replaced by a very large number of equivalent short ones. This means that the blading details can be ignored and only inlet and outlet flow Mach number and direction need be considered. Any information at or around the blade passing frequency must therefore be excluded, but this is much higher than the frequencies associated with entropy fluctuations. The restriction to low frequencies here and in (*a*) above allows rotor blade rows to be treated in exactly the same way as stators after allowing for the change in mean flow Mach number and direction relative to the rotor.

(*c*) Although the entropy and the pressure perturbations are small in relation to the corresponding time mean quantities, the deflexion and acceleration of the mean flow are generally large. This is essential for modelling the phenomenon, since only when the mean flow-changes through a blade row are large does an entropy perturbation produce a significant pressure perturbation.

(*d*) The axial flow is taken to be subsonic. Although this condition could be relaxed, there seems to be no practical interest in turbines with supersonic axial flows.

(*e*) The radial variations along the blades are neglected and the flow is treated as two-dimensional in the developed axial–tangential plane.

(*f*) Although the blades are assumed to be vanishingly short, the overall axial length of the turbine is obtained by allowing appropriate axial gaps between blade rows, and is not necessarily short compared with the relevant wavelengths.

(*g*) The acoustic power produced by the interaction of entropy with the turbine is calculated neglecting the acoustic reflexion from discontinuities downstream of the turbine.

(*h*) When the entropy interacts with the blade row, pressure waves are propagated away from the row upstream and downstream, while vorticity is convected downstream. Because more than one row must be examined, the method is formulated so that the response of each blade row to pertubations in pressure and vorticity, as well as entropy, can be calculated and the effect of coupling blade rows obtained.

In what follows the model is described and the calculation method applied to a number of idealized cases, first isolated blade rows, then isolated stages (stator row and rotor row) and finally to a series of identical stages. From this it is possible to make some broad generalizations.

Finally, the rearward radiated acoustic power of a commercial turbojet predicted with this model is compared with measured values.

2. WAVE STRUCTURE OF THE FIELD

Each of the two-dimensional flow fields, upstream and downstream, of a single compact turbine cascade, is described in the undisturbed state by a constant gas speed, W, in a direction, θ, uniform pressure, p, and density ρ. The two-dimensionality of these fields places no restriction upon area changes within the cascade which occur because of variations in the flow-field depth normal to the x–y plane. The disturbances to this uniform state, which may originate upstream, downstream, or at the cascade itself, consist of two convected waves, the vorticity, $\xi' = \partial v'/\partial x - \partial u'/\partial y$ and the entropy, s', and the acoustic waves; to the first order these waves are independent and, because they do not interact, may be superimposed. Each satisfies the linearized continuity and momentum equations (see figure 2)

$$\frac{D}{Dt}\left(\frac{\rho'}{\rho}\right) + \frac{\partial u'}{\partial x} + \frac{\partial v'}{\partial y} = 0, \tag{1}$$

$$\frac{D}{Dt}(u') = -\frac{1}{\rho}\frac{\partial p'}{\partial x}, \tag{2}$$

$$\frac{D}{Dt}(v') = -\frac{1}{\rho}\frac{\partial p'}{\partial y} \tag{3}$$

and the entropy conservation

$$\frac{D}{Dt}\left(\frac{s'}{c_p}\right) = \frac{D}{Dt}\left(\frac{p'}{\gamma p} - \frac{\rho'}{\rho}\right) = 0, \tag{4}$$

where the operator $\dfrac{D}{Dt} = \dfrac{\partial}{\partial t} + U\dfrac{\partial}{\partial x} + V\dfrac{\partial}{\partial y} : U = W\cos\theta$, and $V = W\sin\theta$.

A plane entropy wave whose normal makes an angle ν_s with respect to the x-axis, with scalar wave number k_s and angular frequency ω, written

$$\frac{s'}{c_p} = \sigma \exp\{i[\omega t - k_s(x \cos \nu_s + y \sin \nu_s)]\} \tag{5}$$

will satisfy equation (4) if the relation

$$(ak_s/\omega) M \cos(\nu_s - \theta) = 1) \tag{6}$$

holds, with $M = W/a$. The entropy wave is accompanied by no velocity field $u'_s = v'_s = 0$, and no pressure field, $p'_s = 0$. The density field associated with the entropy disturbance follows from equation (1) and the second equality in equation (4),
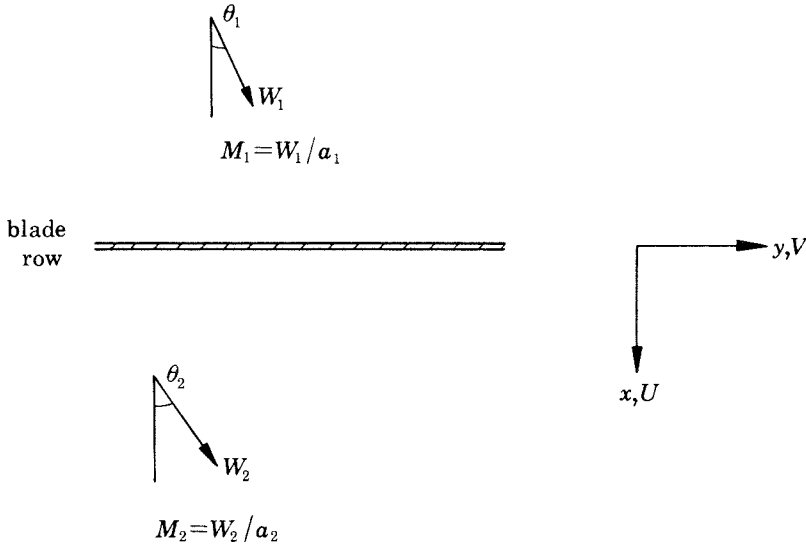
$$\rho'_s/\rho = -s'/c_p. \tag{7}$$

FIGURE 2. Coordinate system.

The vorticity wave, or shear wave, may be written directly after noting that, from equations (2) and (3), $D(\xi')/Dt = 0$. The perturbation vorticity wave may then be written, similar to the entropy wave,

$$\xi' = \xi \exp\{i[\omega t - k_\xi(x \cos \nu_\xi + y \sin \nu_\xi)]\} \tag{8}$$

for a wave with normal direction ν_ξ and scaler wave number k_ξ. These are related to the angular frequency through

$$(ak_\xi/\omega) M \cos(\nu_\xi - \theta) = 1. \tag{9}$$

The vorticity carries no pressure disturbance, with the consequence that $D(u'_\xi)/Dt = D(v'_\xi)/Dt = 0$. Because there is an independent entropy perturbation, no generality is lost in taking $\rho'_\xi = 0$ and therefore the velocity associated with the

vorticity wave is, from equation (1), divergence free. The resulting velocity field may be written as

$$u'_\xi/a = -\mathrm{i}\,(\xi/ak_\xi)\sin\nu_\xi\exp\{\mathrm{i}Z\}, \tag{10}$$

$$v'_\xi/a = \mathrm{i}\,(\xi/ak_\xi)\cos\nu_\xi\exp\{\mathrm{i}Z\}, \tag{11}$$

where $Z \equiv \omega t - k_\xi\,(x\cos\nu_\xi + y\sin\nu_\xi)$. It is more convenient for further analysis to express this as the perturbation in velocity magnitude, $w'_\xi = u'_\xi\cos\theta + v'_\xi\sin\theta$,

$$w'_\xi/a = -\mathrm{i}(\xi/ak_\xi)\sin(\nu_\xi-\theta)\exp\{\mathrm{i}Z\} \tag{12}$$

and the disturbance to flow angle $\theta'_\xi = (-u'_\xi\sin\theta + v'_\xi\cos\theta)/W$,

$$\theta'_\xi = \mathrm{i}(\xi/ak_\xi M)\cos(\nu_\xi-\theta)\exp\{\mathrm{i}Z\}. \tag{13}$$

Because the entropy and vorticity variations are described by independent solutions, the acoustic waves are irrotational and isentropic and satisfy

$$\left(\frac{\mathrm{D}}{\mathrm{D}t}\right)^2\left(\frac{p'}{\gamma p}\right) - a^2\left(\frac{\partial^2}{\partial x^2}+\frac{\partial_2}{\partial y^2}\right)\left(\frac{p'}{\gamma\rho}\right) = 0. \tag{14}$$

The solution with scalar wave number k and wave normal inclined at ν to the axial direction

$$p'/(\gamma p) = p^\nu\exp\{\mathrm{i}[\omega t - k_x x - k_y y]\} \tag{15}$$

satisfies equation (14), provided that

$$\left(1-\frac{ak_x}{\omega}M\cos\theta - \frac{ak_y}{\omega}M\sin\theta\right)^2 - \left(\frac{ak_x}{\omega}\right)^2 - \left(\frac{ak_y}{\omega}\right)^2 = 0, \tag{16}$$

and when the wave number components are real, it is convenient to write $k_x = k\cos\nu$, $k_y = k\sin\nu$. Then the dispersion relation may be written in a form

$$\left\{1-\frac{ak}{\omega}M\cos(\nu-\theta)\right\}^2 - \left(\frac{ak}{\omega}\right)^2 = 0 \tag{17}$$

that will prove useful for geometrical representation. The corresponding velocity follows directly from equations (2) and (3) with the consequence that the velocity and angle perturbations are

$$\frac{w'_a}{a} = \frac{(ak/\omega)\cos(\nu-\theta)}{1-(ak/\omega)M\cos(\nu-\theta)}P^\nu\exp\{\mathrm{i}\alpha_\nu\} \tag{18}$$

and

$$\theta'_a = \frac{1}{M}\frac{(ak/\omega)\sin(\nu-\theta)}{1-(ak/\omega)M\cos(\nu-\theta)}P^\nu\exp\{\mathrm{i}\alpha_\nu\}, \tag{19}$$

where $\alpha_\nu \equiv \omega t - k_x x - k_y y = \omega t - k(x\cos\nu + y\sin\nu)$. Because the acoustic disturbance is isentropic, the density perturbation is

$$\rho'_a/\rho = p'/(\gamma p). \tag{20}$$

The dispersion relation (16) admits complex wave numbers and these are associated with attenuated solutions rather than waves. Because the disturbance will always have a Fourier representation about the turbine periphery, the wave number k_y is real and it will be sufficient to write

$$k_x = k_x^{(1)} + \mathrm{i}k_x^{(2)}.$$

The corresponding pressure disturbance is

$$p'/(\gamma p) = P^{\nu, \pm} \exp\{i[\omega t - (k_x^{(1)} \pm i k_x^{(2)}) x - k_y y]\}. \tag{21}$$

It is convenient to again define a vector $k_x^{(1)} = k^{(1)} \cos \nu$, $k_y = k^{(1)} \sin \nu$, normal to the plane disturbance so that the corresponding velocity and angle perturbations are

$$\frac{w_a'}{a} = \frac{(ak^{(1)}/\omega) \cos(\nu - \theta) + \cos\theta \, [\pm i(ak_x^{(2)}/\omega)]}{1 - (ak^{(1)}/\omega) \, M \cos(\nu - \theta) - M \cos\theta \, (\pm i ak_x^{(2)}/\omega)} P^{\nu, \pm} \exp\{\alpha^{\pm}\} \tag{22}$$

and

$$\theta_a' = \frac{1}{M} \frac{(ak^{(1)}/\omega) \sin(\nu - \theta) - \sin\theta \, (\pm i ak_x^{(2)}/\omega)}{1 - (ak^{(1)}/\omega) \, M \cos(\nu - \theta) - M \cos\theta \, (\pm i \, ak_x^{(2)}/\omega)} P^{\nu, \pm} \exp\{\alpha^{\pm}\}. \tag{23}$$

Expressions in equations (21 – (23) correspond directly to those given in equations (15), (18), (19) when the wave number is real.

Selection of the appropriate set of solutions may be divided into two steps. First, the classification of waves according to their direction of travel so that the appropriate number of radiation conditions may be assigned at each blade row and at points far upstream or downstream. Secondly, the performance of the compact cascade must be expressed in a manner which provides matching conditions between the fields upstream and downstream of the blade row.

3. Classification of the waves

The flow across a turbine cascade may be disturbed by an entropy or vorticity wave convected from upstream or by an acoustic wave originating either ahead or downstream. The resulting interaction with the turbine blade row will generally involve all three types of wave, regardless of the initiating disturbance, each having a common peripheral wave number $k_y = k \sin \nu = k_s \sin \nu_s = k_\xi \sin \nu_\xi$. Thus, from equations (6) and (9),

$$\frac{ak_s}{\omega} \cos \nu_s = \frac{ak_\xi}{\omega} \cos \nu_\xi = \frac{1 - (ak_y/\omega) \, M \sin \theta}{M \cos \theta}. \tag{24}$$

Both the entropy and vorticity waves, which are now determined except for their complex amplitudes σ and ξ, are convected with the flow.

For the acoustic waves, the dispersion relation, equation (16), is quadratic, so that the values of ak_x/ω are

$$\frac{ak_x}{\omega} = \frac{-M \cos\theta \, (1 - (ak_y/\omega) \, M \sin\theta)}{1 - M^2 \cos^2\theta}$$

$$\pm \left\{ \frac{(1 - (ak_y/\omega) \, M \sin\theta)^2 - (1 - M^2 \cos^2\theta)^2 (ak_y/\omega)^2}{(1 - M^2 \cos^2\theta)^2} \right\}^{\frac{1}{2}}. \tag{25}$$

In order to construct solutions one must know whether k_x is real or complex and whether the wave moves upstream or downsteam. The discriminant in equation (25), the value of which answers the first of these questions, has a simple physical
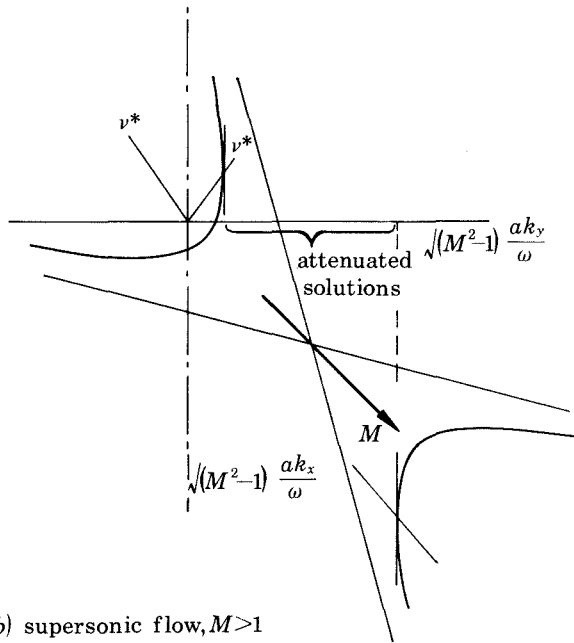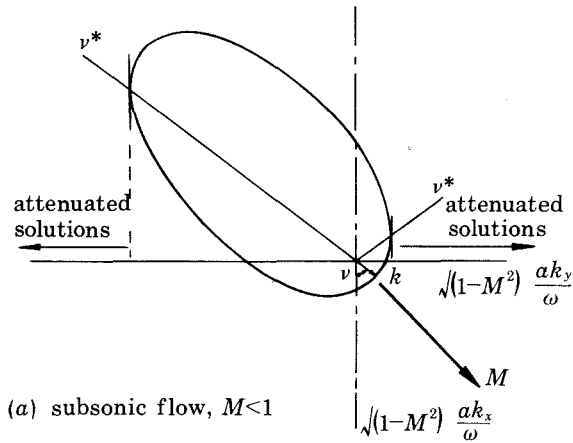
FIGURE 3. Locus of acoustic wavenumber vector for various wave orientations.
(a) Subsonic flow, (b) supersonic flow.

interpretation. An acoustic wave solution with argument $\{\omega t - k_x x - k_y y\}$ has a line of constant phase that moves along the turbine cascade ($x = 0$) with a speed ω/k_y. The gas itself moves with velocity components $W \cos \theta$, $W \sin \theta$ so that the velocity of the constant phase point with respect to the gas is $\{(\omega/k_y - W \sin \theta)^2 + (W \cos \theta)^2\}^{\frac{1}{2}}$; this velocity is supersonic or subsonic depending on whether

$$(1 - (ak_y/\omega) M \sin \theta)^2 - (1 - M^2 \cos^2 \theta)(ak_y/\omega)^2 \tag{26}$$

is positive or negative. The wave front in question may be considered to be generated by a disturbance moving along the turbine cascade so that when its relative velocity is supersonic, an acoustic wave is generated and the radical in equation (25) is real; otherwise, the value of k_x is complex and leads to attenuated solutions.

Since the pressure waves propagate at speed a relative to the gas moving at velocity W the sense of propagation along the turbine axis may be found by considering the sign of the net axial velocity component ($W \cos \theta + a \cos \nu$). The pressure waves move downstream when this is positive and upstream when negative.

The general features of this classification are exhibited geometrically by decomposing the wave number vector parallel to and normal to the stream direction so that $k^2 = (k \cos (\nu - \theta))^2 + (k \sin (\nu - \theta))^2$ and the dispersion relation becomes

$$\left\{ \frac{(1 - M^2)^{\frac{1}{2}} (ak/\omega) \cos (\nu - \theta) + M(1 - M^2)^{-\frac{1}{2}}}{(1 - M^2)^{-\frac{1}{2}}} \right\}^2 + \{(1 - M^2)^{\frac{1}{2}} (ak/\omega) \sin (\nu - \theta)\}^2 = 1.$$

$$(27)$$

For subsonic flow, $M < 1$, this expression represents an ellipse with major axis in the flow direction and symmetry axis displaced upstream a distance $M(1 - M^2)^{-\frac{1}{2}}$; the example in figure 3a gives the wavenumber vector for any orientation ν of the wave normal where the mean flow has a Mach number of 0.85 and is inclined at 45° to the x-axis. The directions ν^* satisfying $M \cos \theta + \cos \nu^* = 0$ also appear in the figure and separate waves that move upstream from those that move downstream. Because the value of ak_y/ω is prescribed, there may be two corresponding values of ak_x/ω, none, or one at each of the extreme values of ak_y/ω. These two extreme values of ak_y/ω occur at the values of ν^* separating the directions of wave motion and are those for which the radical in equation (25) vanishes. Values of ak_y/ω that lie above or below the respective extreme values lead to attenuated solutions. The attenuation is frequently so rapid in the x-direction that waves which are attenuated are generally described as cut-off.

When the Mach number exceeds unity, the quadratic form becomes

$$\left\{ \frac{(M^2 - 1)^{\frac{1}{2}} (ak/\omega) \cos (\nu - \theta) - M(M^2 - 1)^{-\frac{1}{2}}}{(M^2 - 1)^{-\frac{1}{2}}} \right\}^2 - \{(M^2 - 1)^{\frac{1}{2}} (ak/\omega) \sin (\nu - \theta)\}^2 = 1$$

$$(28)$$

and represents a hyperbolic section, the asymptotes of which have slopes $\pm \sqrt{(M^2 - 1)}$. The wavenumber vector may have its terminus on either branch. For the example in figure 3b for $M = 1.15$ and $\theta = 45°$, the values of ak_x/ω corresponding to a given ak_y/ω both lie on the same branch. For large values of ak_y/ω the two values of ak_x/ω lie on the upper branch, the waves facing upstream; for lower values of ak_y/ω the two values of ak_x/ω lie on the lower branch and the waves face downstream. In each case, one wave propagates upstream and the other downstream. Intermediate values of the peripheral wave number ak_y/ω have intersections with neither branch and lead to attenuated solutions. The situation

depicted in figure 3 b is valid for values of the Mach number $1 < M < 1/\cos\theta$, the upper limit corresponding to a sonic velocity component in the axial direction. For $M > 1/\cos\theta$, the lower asymptote has a negative slope, the two solutions for a prescribed ak_y/ω lie on different branches of the hyperbola, real values of ak_x/ω exist for all values of k_y, and there are no attenuated solutions. Because this situation is almost never encountered in practice, discussion will be restricted to the circumstances depicted in figures 3 a or b.

In the present model it is envisioned that the entropy variation from the combustion chamber consists of standing waves in the circumferential sense. It is convenient to resolve this into two equal amplitude travelling waves moving in opposite direction. In general neither the character of the waves nor the response of the blades are the same for waves travelling in the opposing directions and it is therefore necessary to distinguish between those to the left and to the right in the notation of figure 2.

4. CHARACTERISTICS OF THE ACTUATOR DISK

Because the axial extent of the blade row has been assumed infinitestimally small, which was possible because wave lengths that are large in comparison with the actual blade chord are being considered, the characteristics of the cascade constitute matching conditions between the flow fields upstream and downstream of the blade row. Three of the four matching conditions are (i) conservation of entropy, indicating that the perturbations do not change the losses across the cascade, (ii) continuity of mass flow, a statement that the blade row has no capacitance, (iii) conservation of stagnation enthalpy in a coordinate system fixed with respect to the blade row. The fourth condition depends on the blade outlet Mach number. For subsonic flow a condition on the gas efflux angle with respect to the blade row is imposed, while in supersonic outlet flow, a choking condition is used instead. In order to apply these in matching the wave solutions, they will be most conveniently stated in terms of the dimensionless variables $p'/(\gamma p)$, s'/c_p, w'/a, and θ'

Denoting the states ahead of and behind the blade row, by subscripts 1 and 2, the entropy conservation is simply

$$s_1'(0, y, t) = s_2'(0, y, t). \tag{29}$$

If the passages contributed significant losses, such as stall, or contained shocks, this relation becomes complex but may be handled.

The instantaneous equality of mass flow entering and leaving the blade row requires that

$$\frac{\rho_1'}{\rho_1} + \frac{w_1'}{W_1} - \theta_1' \tan\theta_1 = \frac{\rho_2'}{\rho_2} + \frac{w_2'}{W_2} - \theta_2' \tan\theta_2. \tag{30}$$

where again the perturbations are evaluated at the blade row, $\rho_1'(o, y, t)$, etc., and the unperturbed states, ρ_1, W_1, θ_1 and ρ_2, W_2, θ_2 are related by arbitrary cascade

characteristics and area change. It is understood that the W, θ, etc., are measured with respect to the cascade across which the matching is being carried out. The density perturbation in equation (30) may be eliminated in favour of the pressure and entropy changes by using equation (4) in the form

$$\frac{s'}{c_p} = \frac{p'}{\gamma p} - \frac{\rho'}{\rho}, \tag{31}$$

which applies generally to the fields on either side of the cascade. Finally, by eliminating the entropy perturbation and using equation (29),

$$\frac{p_1'}{\gamma p_1} + \frac{1}{M_1}\frac{w_1'}{a_1} - \theta_1' \tan \theta_1 = \frac{p_2'}{\gamma p_2} + \frac{1}{M_2}\frac{w_2'}{a_2} - \theta_2' \tan \theta_2. \tag{32}$$

The conservation of stagnation enthalpy across the blade row implies that the quantity $c_p T + \frac{1}{2}W^2$, is equal at inlet and outlet, a relation conveniently expressed as

$$\frac{1}{1+\frac{1}{2}(\gamma-1)\,M_1^2}\left\{\frac{T_1'}{T_1}+(\gamma-1)\,M_1\,\frac{w_1'}{a_1}\right\} = \frac{1}{1+\frac{1}{2}(\gamma-1)\,M_2^2}\left\{\frac{T_2'}{T_2}+(\gamma-1)\,M_2\,\frac{w_2'}{a_2}\right\}. \tag{33}$$

The temperature perturbation may be elminated by employing the equation of state $p'/p = \rho'/\rho + T'/T$ together with (31) to give

$$\frac{T'}{T} = (\gamma-1)\frac{p'}{\gamma p}+\frac{s'}{c_p}, \tag{34}$$

which, entered into equation (33), yields

$$\frac{1}{1+\frac{1}{2}(\gamma-1)\,M_1^2}\left\{\frac{p_1'}{\gamma p_1} + \frac{s_1'}{(\gamma-1)c_p} + M_1\frac{w_1'}{a_1}\right\}$$
$$= \frac{1}{1+\frac{1}{2}(\gamma-1)\,M_2^2}\left\{\frac{p_2'}{\gamma p_2} + \frac{s_2'}{(\gamma-1)c_p} + M_2\frac{w_2'}{a_2}\right\}. \tag{35}$$

The final matching condition is chosen depending upon whether the discharge velocity relative to the turbine blade row is supersonic or subsonic.

When the discharge velocity is subsonic, then a 'cascade characteristic', such as the discharge flow angle, is the appropriate quantity to prescribe. When the flow leaves the cascade in a direction tangential to the trailing edge, which may be considered the natural limit of the Kutta condition as the blade spacing approaches zero, the condition is

$$\theta_2' = 0. \tag{36}$$

There is no difficulty in using a cascade characteristic $\theta_2' = \text{const }\theta_1'$ when such empirical information is available.

Conversely when the discharge is supersonic (in whcch case the relative inlet velocity is invariably subsonic), there exists a 'throat' within each blade channel,

and they behave as quasi-steady choked nozzles. Then the mass flow per unit area of the cascade plane is proportional to

$$p_1 \, T_1^{-\frac{1}{2}}(1 + \tfrac{1}{2}(\gamma-1) \, M_1^2)^{(\gamma+1)/2(\gamma-1)}$$

and is determined entirely by the approach flow. The fractional variation in mass flow rate rate is

$$\frac{p_1'}{p_1} - \frac{1}{2}\left(\frac{1 + \tfrac{1}{2}(\gamma+1) \, M_1^2}{1 + \tfrac{1}{2}(\gamma-1) \, M_1^2}\right)\frac{T_1'}{T_1} + \frac{\tfrac{1}{2}(\gamma+1) \, M_1^2}{1 + \tfrac{1}{2}(\gamma-1) \, M_1^2}\frac{w_1'}{a_1}, \tag{37}$$

which, in turn, must equal the left hand side of equation (30). If these two expressions are equated, the result after some reduction leads to

$$\frac{\gamma-1}{2}\frac{p_1'}{\gamma p_1} + \frac{1}{2}\frac{s_1'}{c_p} - \frac{1}{M_1}\frac{w_1'}{a_1} + \frac{1 + \tfrac{1}{2}(\gamma-1) \, M_1^2}{1 - M_1^2}\theta_1' \tan\theta_1 = 0. \tag{38}$$

5. METHOD OF SOLUTION

Equations (29)–(38) provide a description of blade row behaviour from which the response can be calculated. Although in principle they could be manipulated algebraically to yield explicit expressions for each output in terms of each input, this is unattractive, particularly when a succession of blade rows are to be treated. Instead the procedure chosen uses the complex matrix handling facilities of a computer.

(a) A single blade row

The variables† $p_-'/\gamma p$, $p_+'/\gamma p$, $s'/c_{p'}$, and ξ'/a are displayed as column vectors V_1 and V_2 on the upstream and downstream sides of a blade row. Equations (29), (30), (35) and either (36) or (38) form the terms of two four-by-four matrices, B_1 and, B_2, containing terms on the upstream and downstream sides respectively, producing $B_1 V_1 = B_2 V_2$. Whether equation (36) or (38) is used depends on the Mach number of the flow leaving the blade row; if the flow is subsonic at outlet, one row of B_2 contains the terms for constant flow leaving angle, whereas if the flow is sonic or supersonic then the same row in B_1 contains the appropriate terms for the constant corrected mass flow. The correspoding row in B_1 or B_2 contains zeros which constitutes a singularity in the matrices and restrict the way in which they can be handled.

A solution requires that the output variables be in terms of the four inputs. The vector for the upstream, V_1, contains three inputs $p_+'/\gamma p$, s'/c_p and ξ'/a, while the upstream going pressure wave, $p_-'/\gamma p$ is an output. Similarly the downstream vector, V_2, contains three outputs $p_+'/\gamma p$, s'/c_p and ξ'/a but the upstream going pressure wave, $p_-'/\gamma p$, is an input. However the terms in B_1 and B_2 associated with the upstream going pressure waves can be readily rearranged‡ so that in the

---

† p_-' and p_+' are the amplitudes of the upstream and downstream propagating pressure waves respectively.

‡ With $p_-'/\gamma p$ occupying the same position in the upstream and downstream vector the rearrangement of matrices B is particularly easy. It consists of exchanging those terms in B_1 and B_2 multiplying $p_-'/\gamma p$, changing the sign of each term as it is exchanged.

vectors all inputs and outputs are collected on the left and right hand sides of the equation
$$B_I V_I = B_O V_O,$$

subscripts I and O referring to input and output respectively. These matrices, B_I and B_O will not normally be singular and B_O may be inverted to give the four outputs in terms of the four inputs.

(b) Several blade rows

Between the blade rows, variations in perturbation phase and amplitude must be accommodated. The expression for the change in phase and amplitude of the pressure, vorticity and entropy perturbations form the terms of a four-by-four diagonal matrix denoted here by T. Since the vorticity and entropy are convected by the mean flow there is no alteration in amplitude, but merely a shift in phase. The pressure waves which are above cut-off will also propagate with only a shift in phase. Below cut-off, however, the change in the pressure amplitude and phase are of the form
$$\exp\{-(ik_x^{(1)} + k_x^{(2)})\,\delta x\},$$

where δx is the axial separation.

It is convenient to first consider two blade rows in the same manner as the isolated row. Across the upstream row

$$B_{u_1} V_{u_1} = B_{u_2} V_{u_2} \tag{39}$$

and across the downstream row

$$B_{d_1} V_{d_1} = B_{d_2} V_{d_2}. \tag{40}$$

The vector V_{u_2} just out of the upstream row can be related to the vector V_{d_1} just before the downstream row by
$$V_{u_2} = T V_{d_1},$$
so that
$$V_{d_1} = (B_{u_2} T)^{-1} B_{u_1} V_{u_1}.$$
This result for V_{d_1} is inserted into equation (40). The resulting square matrix on the left and right linking V_{u_1} and V_{d_1} are then rearranged, just as for the isolated blade row, in order to collect the variables into input and output vectors, $B_I V_I = B_O V_O$. The matrix B_I is then divided by B_O to give the output variables in terms of the inputs.

If more than two blade rows are present, the matrix multiplication is repeated for successive rows until the final blade row has been included when, as before, the matrices are rearranged to give input and output vectors and the final inversion carried out.

6. Acoustic power considerations

In §§4 and 5 the procedure for calculating pressure perturbations (as well as vorticity perturbations) due to entropy pertubations passing through turbines, has been described. In fact the noise nuisance from a jet engine is related more to

the acoustic power propagating downstream from the turbine than to the amplitude of the pressure waves themselves. The acoustic power has been obtained by using the approach of Bretherton & Garrett (1968), according to which the acoustic power crossing a section is given by

$$W = \int_A n_j c_j \frac{p'^2}{\rho a^2} \frac{\omega}{\omega'} \, dA$$

provided the wave system is locally above cut-off. The quantity p' is the root-mean-square amplitude of the pressure fluctuation and $n_j c_j$ is the component of the pressure wave group velocity in a direction normal to the area, A, over which the integration is taking place. The group velocity contains one term due to convection by the flow and another due to the propagation; in the present notation (where the area is normal to the axial direction) $n_j c_j = W \cos \theta + a \cos \nu$. The Doppler-shifted frequency, ω', observed in the frame of reference moving with the flow is

$$\omega' = \omega/[1 + M \cos (\theta - \nu)],$$

where M is the resultant Mach number of the mean flow inclined at θ to the axial. If the annulus area just downstream of the turbine is A, the acoustic power propagated downstream due to either the left or right wave is given by

$$W = (M \cos \theta + \cos \nu)(1 + M \cos (\theta - \nu)) A a p'^2/(\gamma p).$$

If the downstream pressure perturbation is taken to be related to the entropy fluctuation by $(p'_+/\gamma p) = f_{sp} (s'/c_p)$, where f_{sp} is the appropriate term in the output matrix, the acoustic power can be written as

$$W = (M \cos \theta + \cos \nu)(1 + M \cos (\theta - \nu)) f_{sp}^2 (s'/c_p)^2 (\gamma a p A). \tag{41}$$

Although this equation appears to be independent of the frequency, both ν and f_{sp} are strong functions of frequency. The calculation of power from a broad-band entropy input requires an integration with respect to frequency of equation (41) in which s'/c_p is replaced by its spectral density.

7. RESULTS

For any configuration considered, the calculations produce a very large number of results of which it would be impractical to illustrate more than a few. For the left and right hand wave systems, the amplitude and phase of the upstream and downstream going pressure waves and the vorticity wave are calculated for inputs consisting of entropy, vorticity, and upstream and downstream pressure waves. The results shown here will consist of pressure waves due to entropy wave inputs and the pressure waves reflected or transmitted for an incident pressure wave. The inclination of the waves and the consequent blade row response are frequency dependent. In presenting the results it is convenient to take fY/a as the independent variable,† where f is the frequency in hertz, Y is the wavelength along the cascade

† The variable fY/a is the reciprocal of ak_y/ω used in §§2 and 3. It is used because graphical presentation of results is made easier.
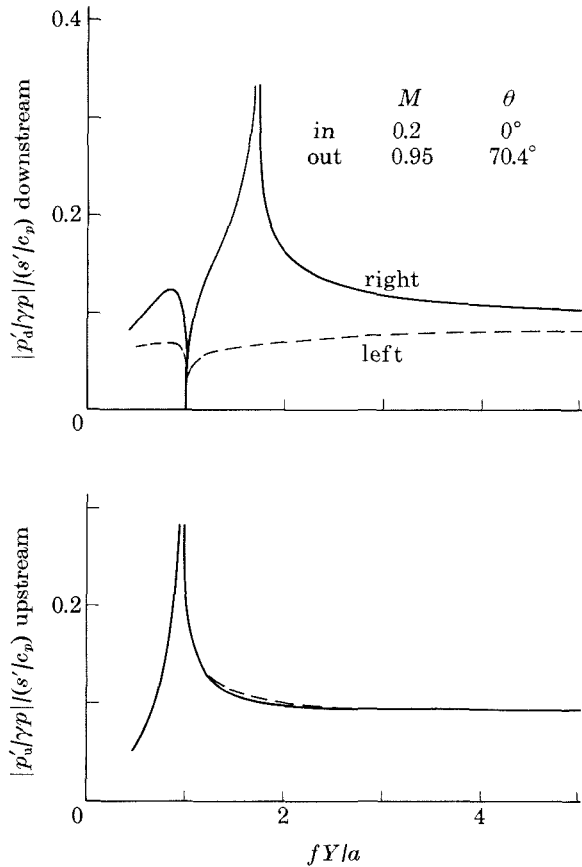
FIGURE 4. Pressure-wave amplitudes due to an entropy wave into an isolated row of nozzle guide vanes with subsonic outlet velocity.

and a is the speed of sound in the flow into the blade row (into the first blade row if there is more than one). When more than one blade row is being considered the axial spacing δx must be specified, and it is physically more relevant to use $\delta x/Y$. In the first part of this section some results obtained from isolated blade rows are examined, in the second part a few results from combinations of blade rows are given, and in the last a calculation for a real engine.

(a) Isolated blade row

Figure 4 shows the ratios of the pressure perturbation amplitude to the entropy amplitude for the upstream and downstream sides of a blade row. The blade row typifies a nozzle guide vane (n.g.v.) with a low Mach number, axial inlet flow and a high subsonic outlet flow, $M_2 = 0.95$, inclined at a large angle to the axial, $\theta_2 = 70.4°$. For the sake of definiteness the height of the blade is assumed constant and it is this which determines the interrelation of Mach number and flow direction. The peak in the upstream and downstream pressures occurs at the point of cut-off

for that region and that wave. Upstream of the blade row, where the flow is axial, the cut-off value of fY/a is identical for the left and right hand wave systems. The cut-off peak on the upstream side produces a trough on the downstream side. The downstream peak in the right hand wave barely produces any effect upstream, however, and this can be explained by the high outlet Mach number reducing the influence of downstream conditions. The calculations very close to the peaks and trough associated with cut-off become relatively inaccurate. It is inferred that the analysis predicts infinite amplitude at the peak, and zero in the trough, but this is, in any case, a consideration of purely academic interest. The results for the supersonic outlet counterpart of the blades described above, with the same inlet conditions and outlet flow angle, but with the outlet Mach number increased to 1.05, are very similar, but the magnitudes are slightly greater. Because the downstream conditions can have no upstream effect when the outflow is supersonic, there is no detectable influence on the upstream side of the peak around the downstream cut-off of the right hand wave.

Calculations have been performed to compare the downsteam pressure wave amplitudes due to entropy wave inputs for a range of blade deflexions and accelerations, in each case taking the blading to be of constant height. It was found that the amplitudes are decreased if the inlet Mach number is raised or the outlet Mach number reduced. A non-axial flow at inlet does not appear to have a significant effect other than to alter the behaviour near to the cut-off condition on the upstream side. In summary it appears that the overriding effect in determining the amplitude of pressure waves produced by entropy interactions with a blade row is the magnitude of the acceleration of the flow through the row. Pickett (1975), using a model based on similar assumptions, has found that the acoustic intensity is approximately proportional to the square of the blade row pressure drop, which is equivalent to the pressure perturbation being proportional to pressure drop.

Figure 5 shows the response of the subsonic blade row used in figure 4 for entropy wave input when exposed to a downstream-going pressure wave. The shape of the variation in amplitude of the transmitted, downstream-going wave with respect to fY/a, is very similar to the variation observed with an entropy wave input but the amplitudes are much larger. The reflected wave however, shows quite a different character with a trough at the upstream cut-off frequency.

Attention was drawn to the significance of the flow acceleration in producing pressure waves from entropy perturbations. In test cases where there was no overall flow acceleration through the blade row, the entropy was found, as expected, to produce no pressure or vorticity waves. This was even true of impulse type blades with large flow deflexion ($\theta_1 = -\theta_2$) but equal inlet and outlet Mach number. Pressure or vorticity waves incident on non-accelerating blade rows do, however, produce new pressure and vorticity waves. Figures 6 compares the present method with calculations by Kaji & Okazaki (1970) of the transmitted and reflected pressure wave amplitudes for an upstream pressure wave incident on an uncambered cascade staggered at 60°. The calculations by Kaji & Okazaki take into account

the finite chord length and pitch in satisfying the boundary conditions on the blades. While the agreement between their method and the present short chord and pitch method is remarkable and not completely understood, it is not altogether surprising in view of the small effect of wavelength to chord ratio, found by Kaji & Okazaki.
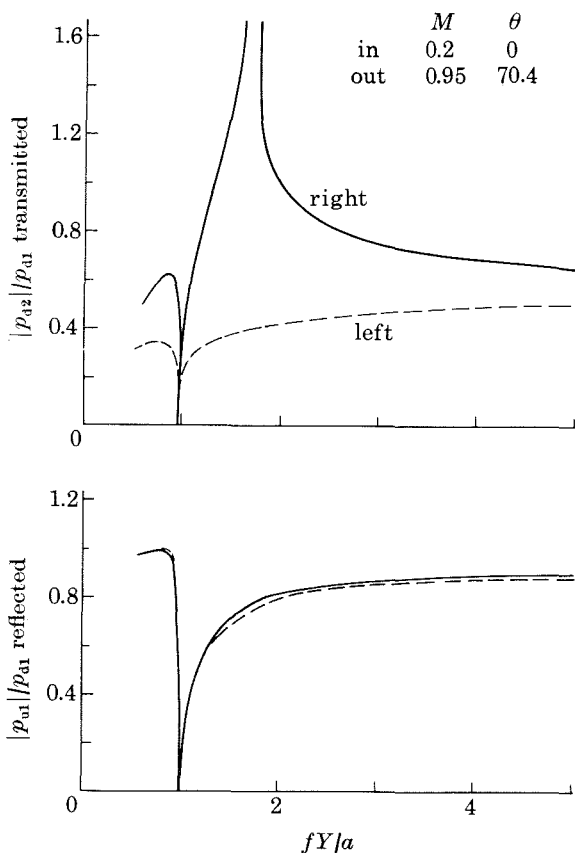

FIGURE 5. Transmitted and reflected pressure-wave amplitudes for downstream-going pressure wave into a subsonic nozzle guide vane row.

The special case of no deflexion or acceleration has been considered above. In another special case the flow remains axial but is accelerated by, for example, a variation in the blade height (normal to x and y). When fY/a tends to infinity, the wave fronts become parallel to the y direction and the model then represents plane waves through a straight, one-dimensional nozzle. The response of a very short one-dimensional nozzle due to small amplitude entropy or pressure perturbations can be analysed very simply (Marble 1973; Marble & Candel 1977) and comparison with calculated response of extended supersonic nozzles (Candel 1972) established the frequency range of good approximations. Sample calculations showed perfect agreement between the one-dimensional analysis and the present method taking $fY/a = 100$.

(b) Several blade rows

The range of possible test cases rises alarmingly with the introduction of several blade rows and only a very few examples are shown here.

Figure 7 shows the downstream pressure wave amplitude due to entropy waves entering a single turbine stage consisting of a row of nozzles followed by a rotor. The blade passages have constant height and the nozzle blades are those used for figure 4, with an axial inlet flow at a Mach number of 0.2 and an outlet Mach number of 0.95. The results of figure 7 are for two different axial spacings differing by a factor of ten, and at the larger there is clear evidence of axial
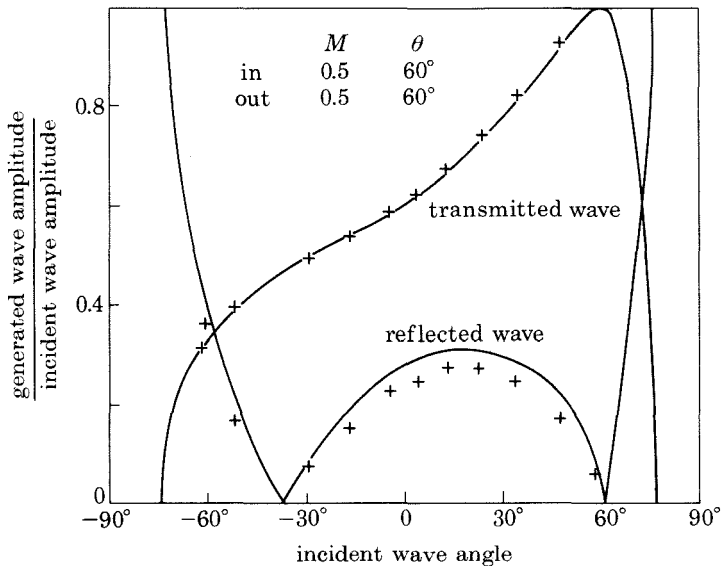

FIGURE 6. Comparison of transmitted and reflected pressure wave amplitudes calculated by present method and by Kaji & Okazaki. For row of uncambered blades with zero thickness. ———, Results of Kaji & Okazaki (space cord ratio = 1), reduced frequency, $\omega c/u = \frac{1}{2}\pi$. +, Results of present calculation.

resonance effects. Although this axial spacing, $\delta x/Y = 0.32$, is larger than a typical turbine stage, in calculations for real multistage turbines with up to 10 blade rows, the overall axial length does become large and such effects have been noticed. Compared with the results for the nozzle row alone (figure 4) it will be seen that the levels are considerably higher for the stages. Furthermore the higher downstream pressure amplitudes were found with the right hand waves for the nozzle whereas the situation is reversed for the stage, with the left hand waves generally having higher amplitudes.

Calculations have been performed to find the effect of turbine loading denoted by $\Delta h_0/U_2$ where Δh_0 is the stage drop in stagnation enthalpy and U is the blade speed. The two stages considered had different rotors but the same stators. A very
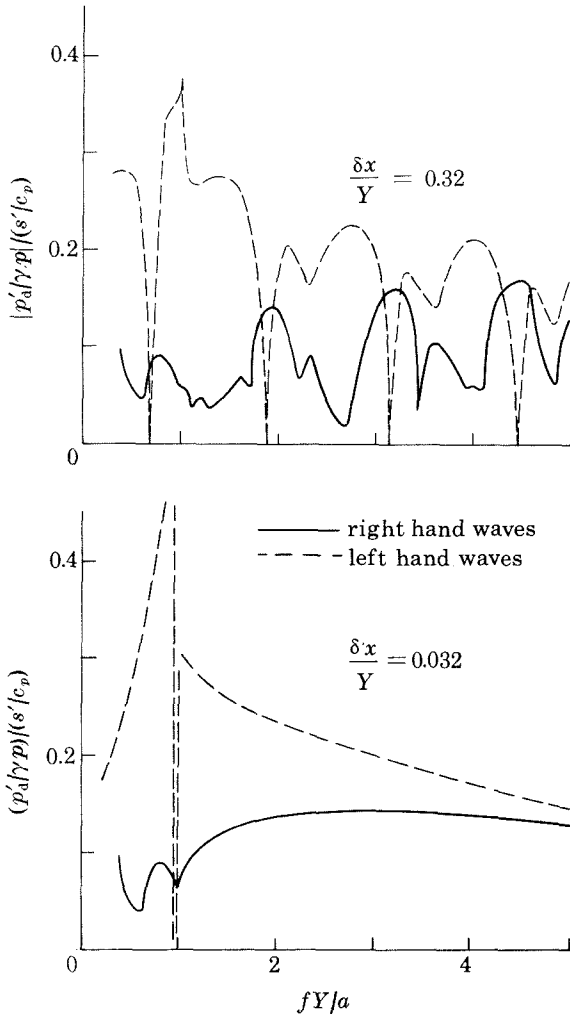
FIGURE 7. Downstream pressure-wave amplitude due to entropy into turbine stage; effect of spacing between n.g.v. and rotor.

strong dependence on turbine loading of the pressure amplitude due to incident entropy was evident. This is consistent with the isolated blade row results in which it was found that the pressure amplitude rose sharply if the mean flow acceleration or mean pressure drop was increased.

Whereas the previous figures showed the spectra or pressure amplitude, figure 8 shows the spectra of downstream acoustic power due to entropy waves into the nozzle guide vanes alone and into a fairly heavily loaded stage. It can be seen that a proper representation of even a single-stage turbine cannot ignore the strong interaction between the rows. For the left hand waves from the full stage and the right hand waves of the nozzles, it is possible to see a quite common trend in plots of power against frequency. The power rises quite rapidly as fY/a is reduced,

until, just before the point of cut-off, there is a precipitous fall. Although the pressure amplitude at the point of cut-off, figure 7, appears to be infinite, the orientation of the waves is such that no power is actually transmitted.

Most jet engines have several turbine stages and to investigate this the spectra of non-dimensional acoustic power due to an entropy perturbation into turbines with different numbers of stages were calculated. The stages all had 50% reaction and 'repeat', that is to say the flow Mach numbers and directions are the same for each stage. The fall in temperature across each stage, however, leads to a drop
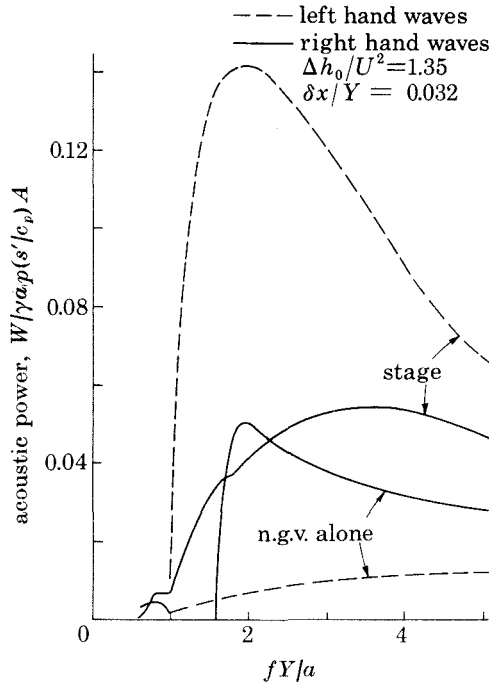

FIGURE 8. Downstream acoustic power due to entropy wave into isolated nozzle guide vane row and into a turbine stage.

in the acoustic velocity, and for this reason the cut-off value of fY/a at outlet falls with the number of stages. The power curves again showed the tendency to rise with fall in fY/a followed by the precipitous drop at the point of cut-off. The peak spectral density of acoustic power increased with the number of stages with a shift towards lower values of fY/a. The integral of the power with respect to frequency was found, however, to be virtually constant for two or more stages.

(c) A calculation for an engine

Figure 9 shows a comparison for a commercial turbojet engine between measured rear arc overall acoustic power in the frequency range 20 Hz to 1 kHz and the predictions of the present model.

The engine used for this comparison, a Pratt and Whitney JT8D-9, was selected

because of the relatively complete aerodynamic, combustion chamber and acoustic data available. The blade aerodynamic data was taken at the mid annulus height. The combustion chamber data has been measured in a similar engine (see Picket 1975); from this the root mean square entropy level was approximated by $s'/c_p = 2\%$ and its spectrum by a linear drop of 16 dB between 20 Hz and 1 kHz.

The model does not consider effects of the acoustic transmission through the final engine nozzle. Unfortunately, no method for handling this was available and the effects have been ignored. The measured noise does not show spectral peaks thought to be associated with reflexions from the nozzle and the effect is probably less serious than it might at first appear.
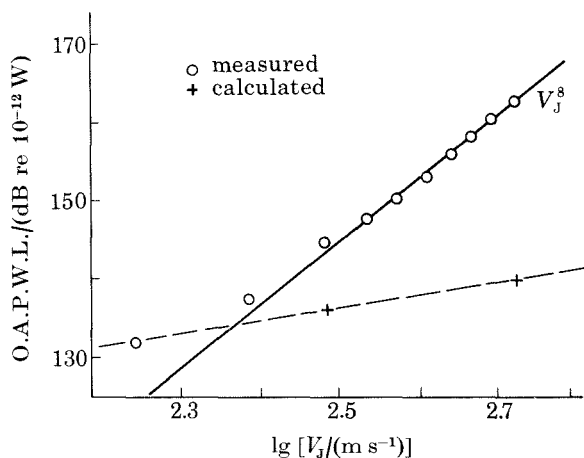

FIGURE 9. Predicted and measured rear arc overall acoustic power (O.A.P.W.L.), 20 Hz to 1 kHz, for JT8D-9 engine.

The calculated acoustic powers shown in figure 9 correspond to an aircraft at take-off and at approach. It is when the jet velocity is low that the present mechanism appears most significant, and at very low velocities its level is even higher than the jet mixing noise (proportional to V_J^8). The model does seem to predict the usual trend in noise at low jet speeds (figure 1). In fact the variation in the predicted noise with jet velocity is approximately equal to $V_J^{1.5}$, very typical of measured trends at very low velocities. The application of this model to the prediction of engine noise levels is considered in greater detail by Cumpsty & Marble (1977).

8. CONCLUSIONS

From the idealized cases considered it has been found that the pressure wave amplitudes, produced by an entropy wave interacting with an isolated blade row, increase with the degree of flow acceleration through the row, although the overall behaviour was not very different for blades with subsonic or supersonic outlet velocities. The short blade model appeared to match the behaviour predicted for

the reflexion and transmission of pressure waves by an analysis taking account of blade chord and pitch.

For a stage, pressure amplitude and power due to entropy perturbations also increased with stage loading and were markedly higher for a stage than a nozzle guide vane row alone. Finally, the acoustic power from two identical stages was greater than for one stage and, although aditional identical stages shifted the spectrum to lower frequencies with a higher peak, the overall power did not increase any further in the example considered.

The level of predicted acoustic power, and its trend with jet velocity, appear to agree very well with those measured on a commercial turbojet engine.

REFERENCES

Bretherton, F. P. & Garrett, C. J. T. 1968 *Proc. R. Soc. Lond.* A **302**, 524–554.

Candel, S. M. 1972 Analytical studies of some acoustic problems of jet engines. Ph.D. dissertation, California Institute of Technology.

Cumpsty, N. A. & Marble, F. E. 1977 Core noise from gas turbine exhausts. *J. Sound Vibr.* **54**. (To be published.)

Dils, R. R. 1973 *Trans. Am. Soc. mech. Engrs* A; *J. Engng Power* **95**, 265–277.

Hoch, R. & Hawkins, R. 1973 Recent studies in Concorde noise reduction. AGARD Conference Proceedings, CP-131, *Noise Mechanisms*.

Kaji, S. & Okazaki, T. 1970 *J. Sound Vibr.* **11**, 355–375.

Marble, F. E. 1973 Acoustic disturbance from gas nonuniformities through a nozzle. *Proc. Interagency Symp. Univ. Res. Transp Noise*, Stanford University, June 1973, vol. 3.

Marble, F. E. & Candel, S. M. 1977 Acoustic disturbance from gas non-uniformities convected through a nozzle. *J. Sound Vibr.* **55**. (To be published).

Matthews, D. C. & Perachio, A. A. 1974 Progress in core engine and turbine noise technology *American Institute of Aeronautics and Astronautics 6th Aircraft Design, Flight Test and Operations Meeting*, Los Angeles, California, August 1974, paper no. 74-948.

Pickett, G. F. 1975 Core engine noise due to temperature fluctuations convecting through turbine blade rows. *American Institute of Aeronautics and Astronautics 2nd Aero-Acoustics Conference*, Hampton, Virginia, March 1975, paper no. 75–528.